

Green Modification of Iron Oxide Nanoparticles with *Achillea wilhelmsii* and Investigation of Their Performance for Methylene Blue Adsorption

Zahra Pourmanouchehri^{a,b}, Azam Chahardoli^{c,b}, Farshad Qalekhani^{a,b}, Hossein Derakhshankhah^b, Yalda Shokoohinia^{a,d}, Ali Fattahi^{a,b*}, Alireza Khoshroo^{a,b*}

^a Department of Pharmaceutics, Faculty of Pharmacy, Kermanshah University of Medical Sciences, Kermanshah, Iran.

^b Pharmaceutical Sciences Research Center, Kermanshah University of Medical Sciences, Kermanshah, Iran.

^c Department of Biology, Faculty of Science, Razi University, Kermanshah, Iran.

^d Ric Scalzo Botanical Research Institute, Southwest College of Naturopathic Medicine, Tempe, AZ, USA

Corresponding authors:

Alireza Khoshroo
Pharmaceutical Sciences Research Center, Kermanshah University of Medical Sciences, Kermanshah, Iran
E-mail addresses: khoshroo.a.r@gmail.com

Ali Fattahi
Medical Biology Research Center, Kermanshah University of Medical Sciences, Kermanshah, Iran
E-mail addresses: alifattahi@kums.ac.ir

Table S1Antioxidant activity of *Achillea wilhelmsii C. Koch* extract at different concentration

<i>Achillea wilhelmsii C. Koch aqueous extract (mg/mL)</i>	% DPPH radical scavenging effect
50	27.04± 0.75
100	59.39± 1.01
150	79.52± 2.17

Table S2. Comparison of the adsorption capacity (q_e) of the Aw- Fe_3O_4 NPs to that of already known Fe_3O_4 NPs adsorbent.

Adsorbent	Particles size (nm)	Surface area (m ² /g)	Organic dye	Adsorption capacity (mg/g)	references
Alg- Fe_3O_4	12	-	Malachite green	13.76	[1]
$\text{Fe}_3\text{O}_4@\text{PDA}$	340	-	Methylene blue	10	[2]
$\text{Fe}_3\text{O}_4@\text{GTPs NPs}$	13.5	-	Methylene blue	7.25	[3]
Z. a. Fe_3O_4 NPs	17	-	Methylene blue	3.55	[4]
Fe-AC	-	940.132	Methylene Blue	370.4	[5]
Fe_3O_4 -AC	-	389.23	Malachite green	311.40	[6]
Coal fly ash	-	2.6991	Methylene Blue	0.12	[7]
γ - Fe_2O_3	38–45	81.61	Malachite green	227.3	[8]
Fe_3O_4	10	170	Methylene Blue	185.5	[9]
Aw- Fe_3O_4 NPs	18	32.63	Methylene blue	7.91	This work

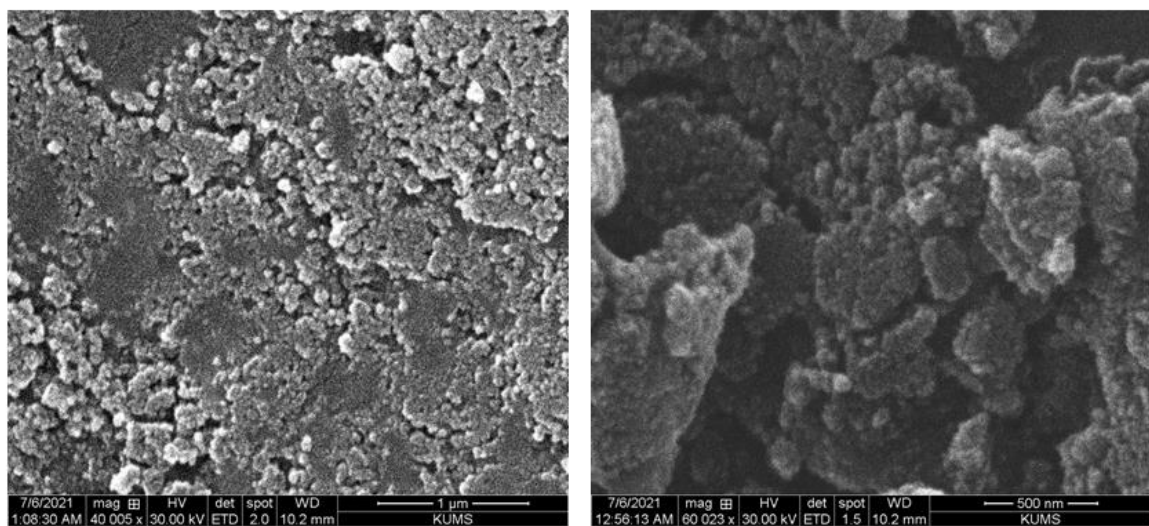


Fig. S1. SEM images of Aw-Fe₃O₄ NPs

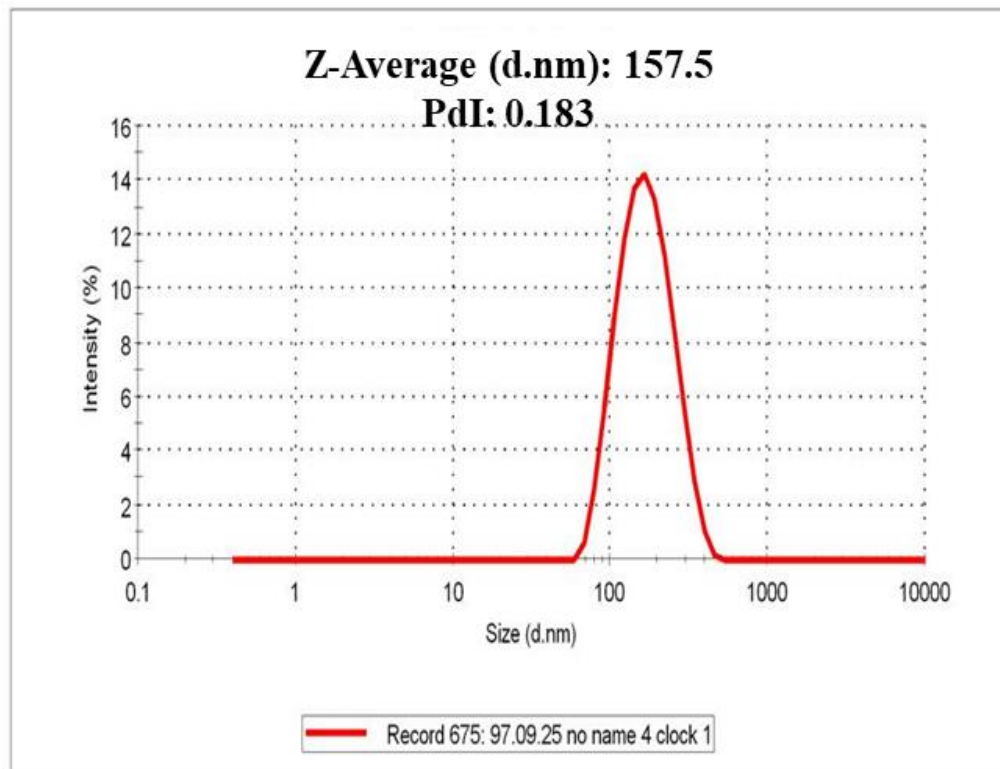


Fig. S2. Dynamic light scattering (DLS) of the Aw- Fe_3O_4 NPs.

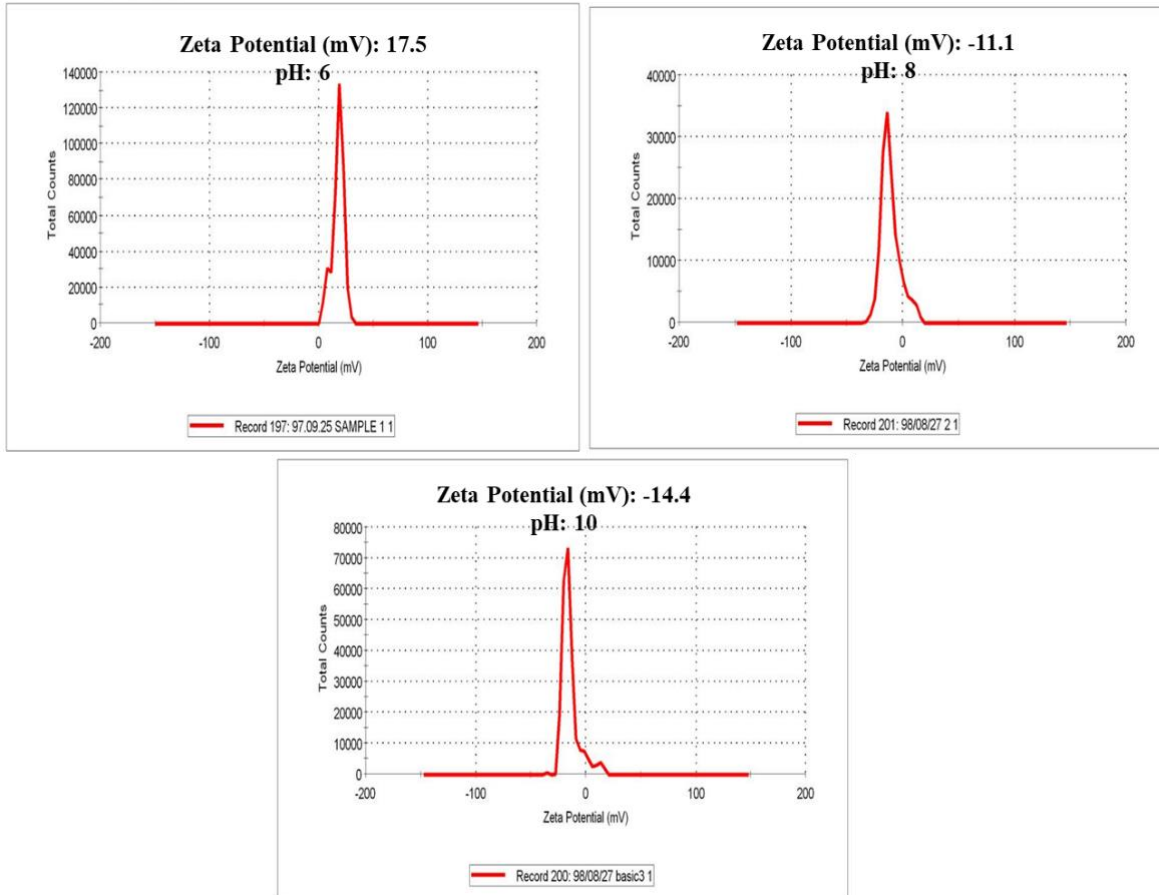


Fig. S3. Zeta potential analysis of the Aw- Fe_3O_4 NPs at; pH: 6, pH: 8, pH: 10.

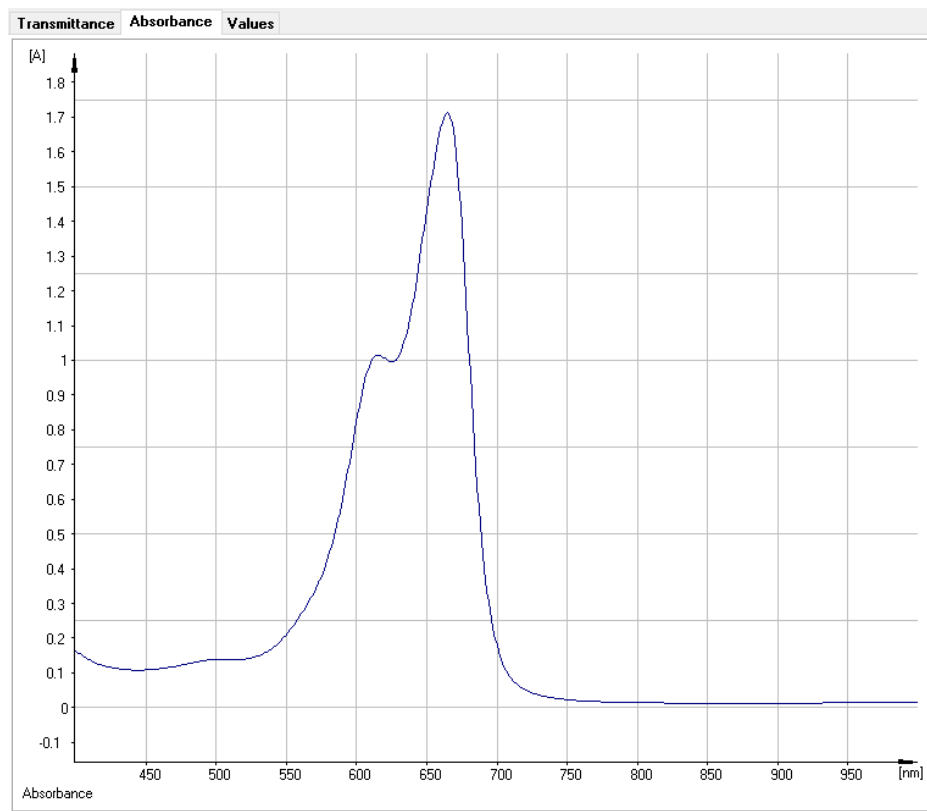


Fig. S4. The UV-vis spectra of MB (30 ppm).

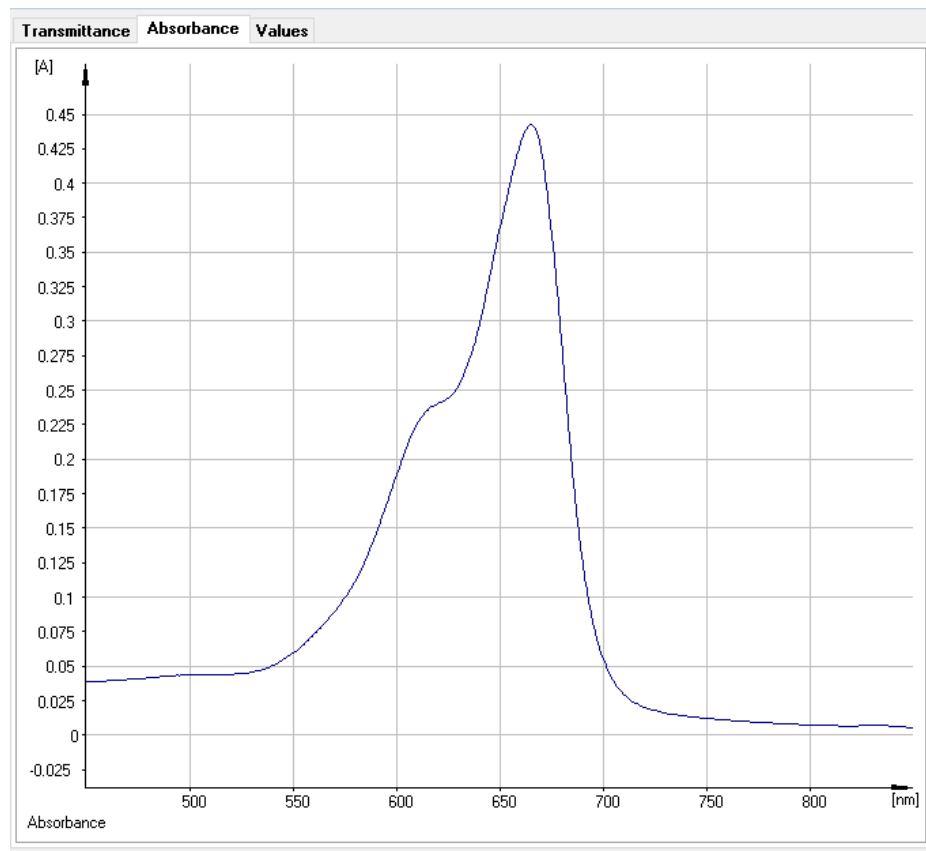


Fig. S5. The UV-vis spectra of MB after exposure to Aw- Fe_3O_4 NPs (pH 11, 30 ppm, 120 min).

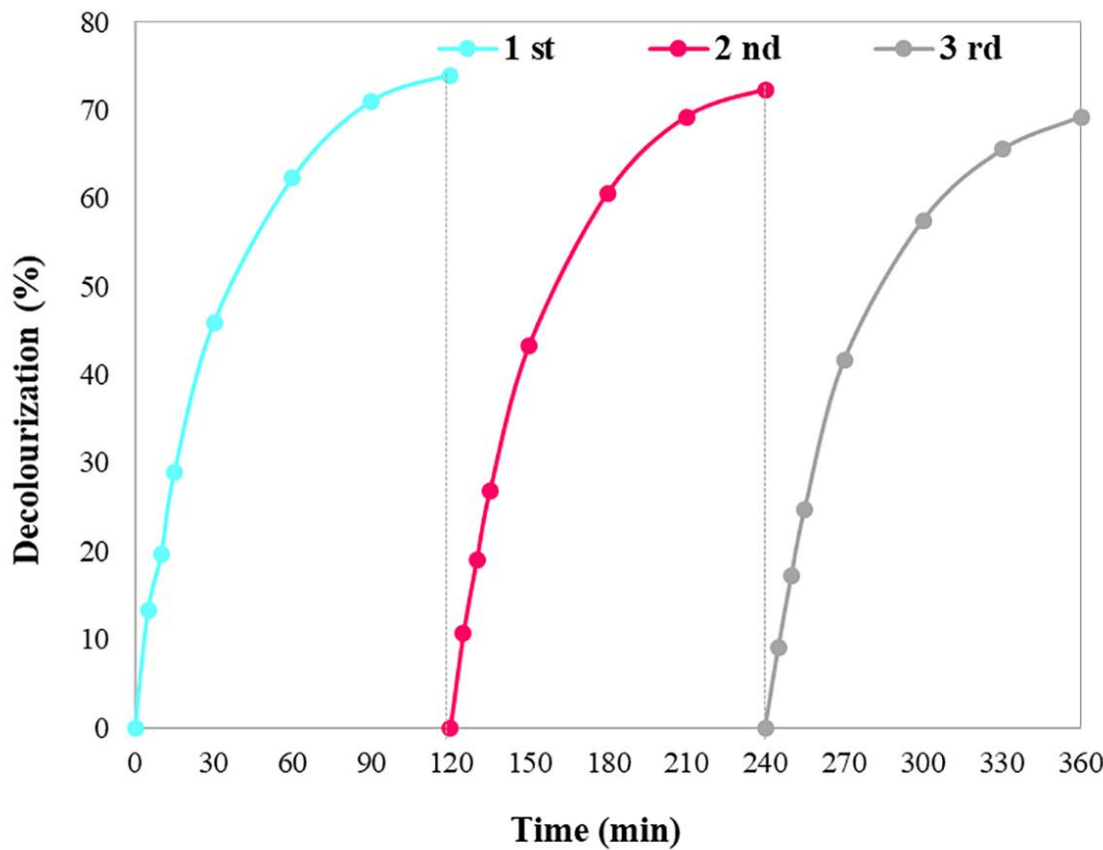


Fig S6. Catalytic reusability of the Aw-Fe₃O₄ NPs for adsorption of MB for three cycling runs.

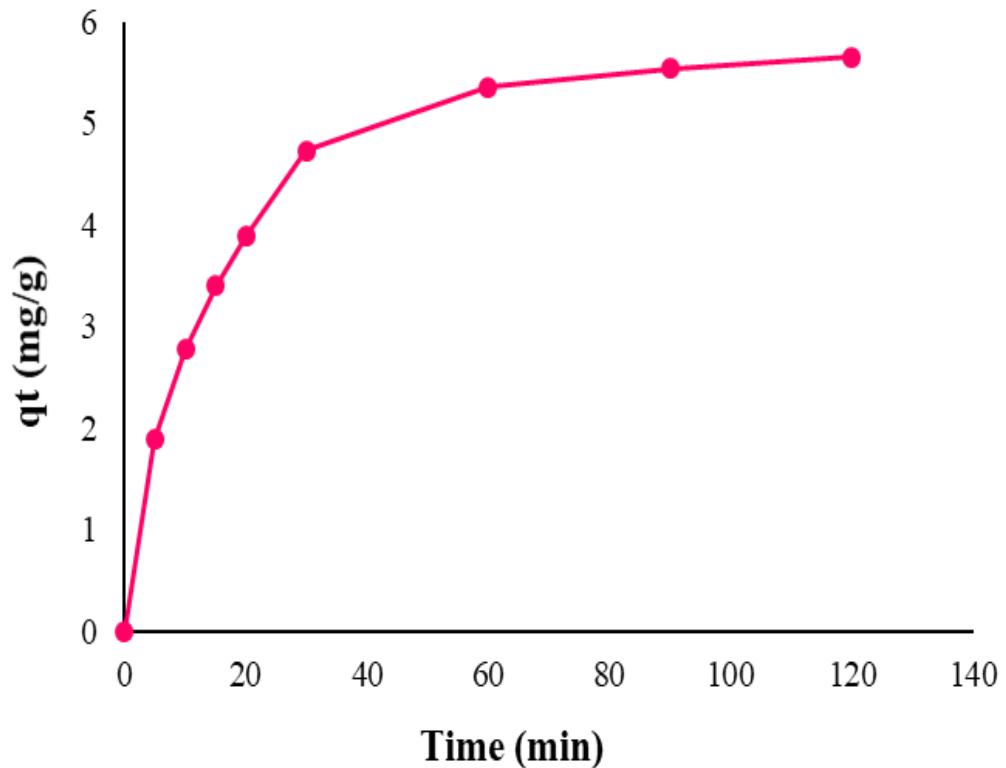


Fig S7. Effect of contact time on the adsorption of MB on Aw- Fe_3O_4 NPs.

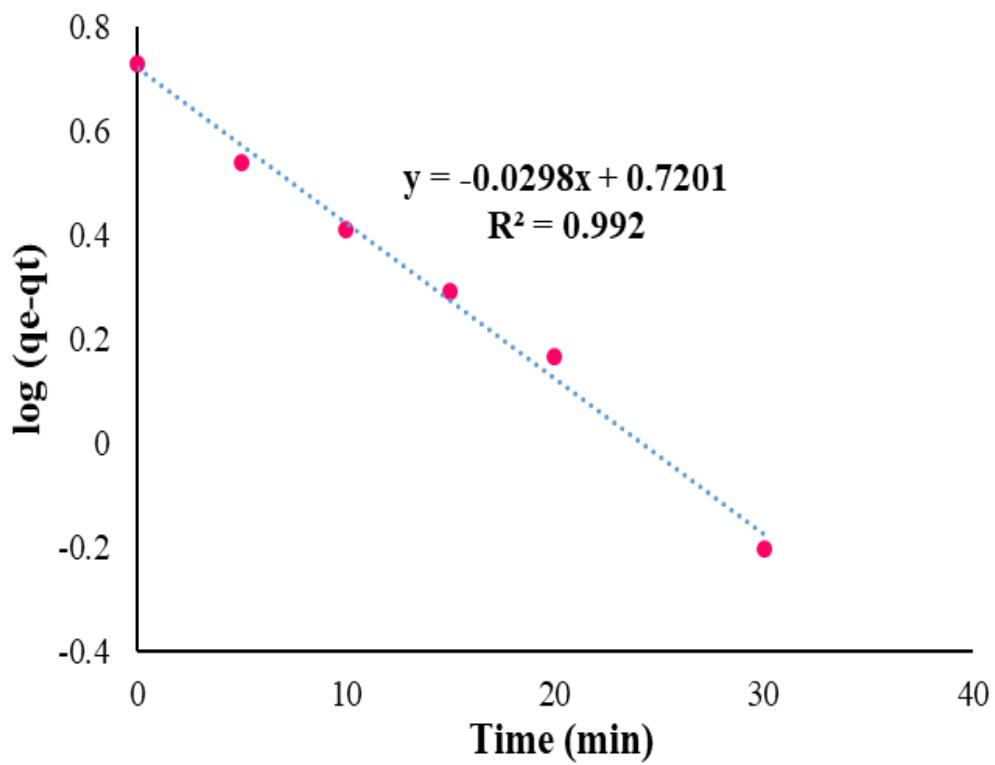


Fig S8. Pseudo-first order plots for the adsorption of MB onto the Aw- Fe_3O_4 NPs.

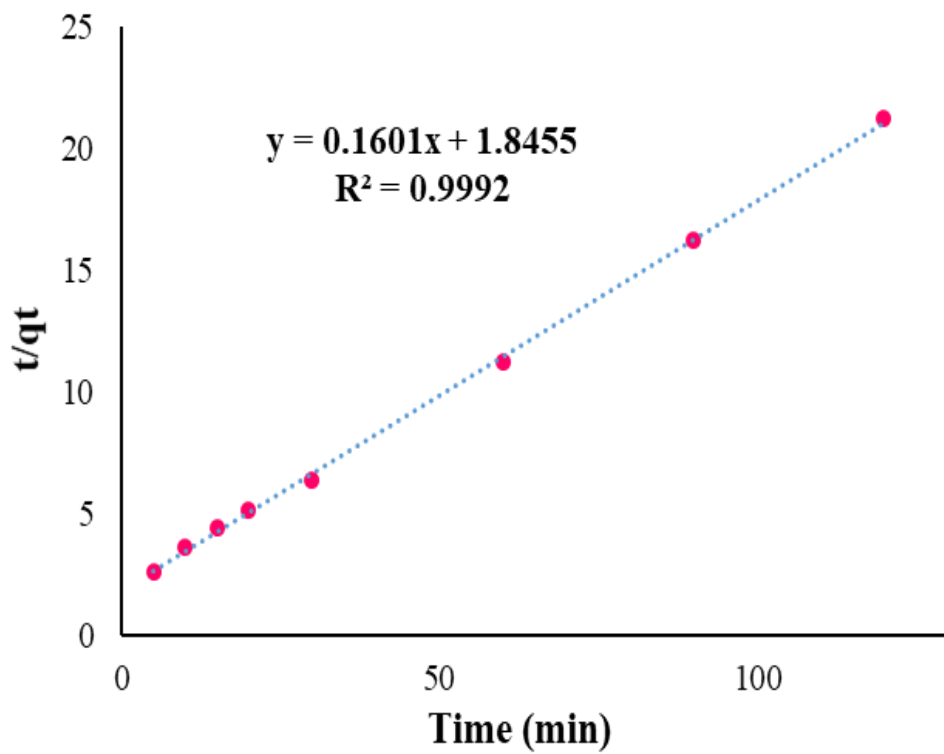


Fig S9. Pseudo-second order plots for the adsorption of MB onto the Aw- Fe_3O_4 NPs.

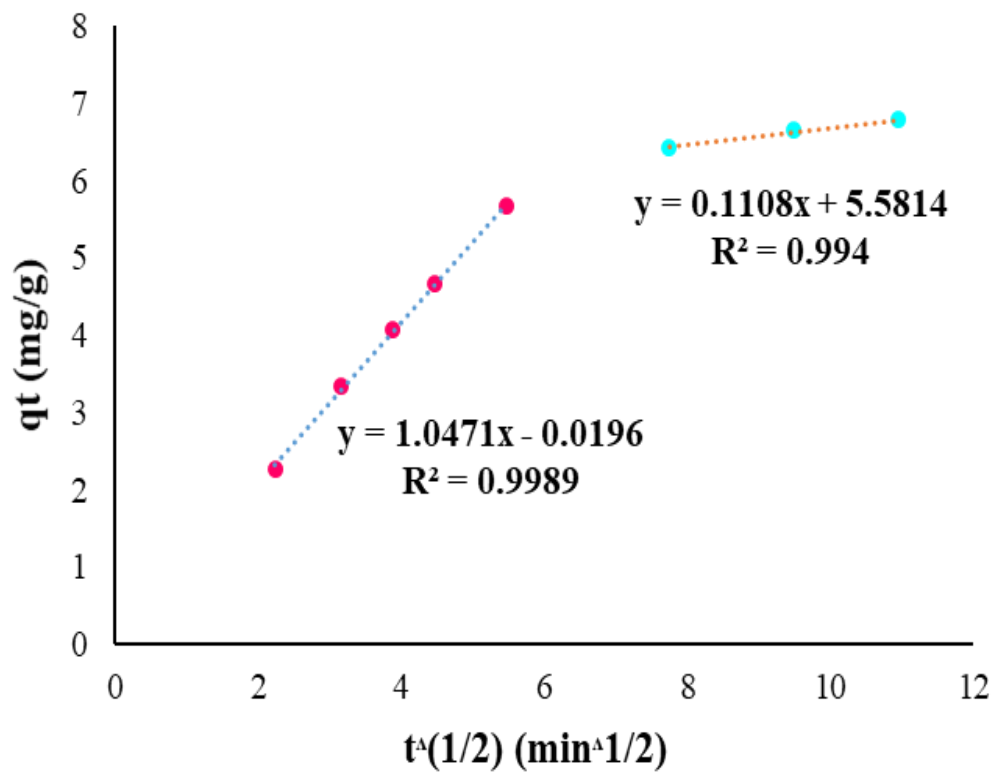


Fig S10. Intraparticle diffusion plots for the adsorption of MB onto the Aw-Fe₃O₄ NPs.

Reference

1. A. Mohammadi, H. Daemi, and M. Barikani, *Int. J. Biol. Macromol.* **69**, 447 (2014).
2. Z. Zhou and R. Liu, *Colloids Surfaces A Physicochem. Eng. Asp.* **522**, 260 (2017).
3. K. K. Singh, K. K. Senapati, and K. C. Sarma, *J. Environ. Chem. Eng.* **5**, 2214 (2017).
4. A. V Ramesh, D. Rama Devi, S. Mohan Botsa, and K. Basavaiah, *J. Asian Ceram. Soc.* **6**, 145 (2018).
5. E. Altintığ, H. Altundag, M. Tuzen, and A. Sarı, *Chem. Eng. Res. Des.* **122**, 151 (2017).
6. E. Altintığ, M. Onaran, A. Sarı, H. Altundag, and M. Tuzen, *Mater. Chem. Phys.* **220**, 313 (2018).
7. H. Karaca, E. Altintığ, D. Türker, and M. Teker, *J. Dispers. Sci. Technol.* **39**, 1800 (2018).
8. A. Afkhami, R. Moosavi, and T. Madrakian, *Talanta* **82**, 785 (2010).
9. B. Khan, M. Nawaz, M. Waseem, R. Hussain, S. Arif, G. J. Price, S. Haq, and W. Rehman, *Mater. Res. Express* **6**, 95511 (2019).